An experimental study on high-pressure pulsed sprays for efficient management of high heat fluxes for moderate area devices

1st Fernando Soria, 2nd Edward Woodruff, 3rd Andrew Fordon, 4th Shawn A. Putnam, 5th Yunjun Xu Department of Mechanical and Aerospace Engineering, University of Central Florida, Orlando, FL 32817, USA fsoria0408@knights.ucf.edu, grant.woodruff@knights.ucf.edu

Abstract—This work showcases an experimental subsaturation spray cooling setup for a range of heat fluxes from 0.93 W/cm² to 4.66 W/cm². The system consists of a 12" Aluminum square heat source unit with 28 embedded 1800 W cartridge heaters. An external high-pressure air tank provides the system with spraying pressures ranging from 500 to 3000 Psi. Userdefined control algorithms command four piezoelectric actuated injectors allowing for the manipulation of the spray frequency, duration, duty cycle, and coordination between multiple piezoinjectors. Thus far, experiments in the horizontal configuration have shown that at 60°C, surface temperatures for all heat fluxes prove difficult to control. At 90°C, however, successful results show that heat fluxes of 1.86 W/cm² and 2.79 W/cm² are sustainable. Conducting experiments at aggressive power loads and surface temperatures significantly below saturation introduce spray-pooling, coolant pools which inhibit the evaporation rate, significantly diminishing the spray cooling efficiency. To counteract this effect, additional experiments were performed in a vertical configuration to avoid the pooling of non-evaporated coolant and enhance the heat transfer through the falling film. The results show surface temperature control for 60°C and 90°C within 6°C of the average surface temperature for heat fluxes up to 0.93 W/cm² and 3.72 W/cm², respectively.

Index Terms—Spray Cooling, Pulsation, Evaporation, Two-Phase

I. INTRODUCTION

In recent years, rapid advancements in computer chips, satellites, and a vast array of other technologies have led to an influx of cooling problems due to increased power draw and higher generated heat flux. Thus, an efficient, high heat flux thermal control system must be established. For example, a targeted application of this solution is in data centers where the power draw can surpass 1 MW. This application presents a particularly difficult problem as computer hardware such as hard disk drives (HDDs), microprocessors, and dual inline memory modules (DIMMs) must be kept at specific subsaturation operating temperatures of 60°C and 90°C respectively to ensure the stability and longevity of components. The 2004 iNEMI electronics manufacturing initiative technology roadmap outlines the trend in chip power and heat flux over time, and thus far has been a very accurate predictor. If the trend indicated by the roadmap continues, we could see heat fluxes surpassing 200 W/cm² by 2020 [5]. There have been

This work was supported by the National Science Foundation (NSF) [grant number: 2032764]

several proposed solutions to dissipate these high heat fluxes including jet impingement, single-phase microchannels, and spray cooling. Jet impingement, while it can keep up with the increased generated heat fluxes of high-power electronics, is only viable in cooling isolated hotspots as opposed to a larger area [1]. This pinpoint cooling results in non-uniform surface temperatures, diminishing its effectiveness in most applications. Additionally, a study conducted in 1998 [2] found that while jet impingement and spray cooling can achieve similar heat transfer rates, spray cooling utilizes a mass flux an order of magnitude less than that of its counterpart.

Like jet impingement, single-phase microchannel cooling targets centralized heating loads across small areas. According to Lee and Vafai [3] the ideal heating area for microchannel cooling is under 49cm² (0.07 by 0.07m). Regardless, past experimental results have shown promising results thus far dissipating power densities as high as 3000W/cm² for single-phase flow [4]. These described methods are sustainable for their own specific applications and specialized use cases. This work will focus on the sub-saturation cooling of larger areas (929 cm²), by utilizing multi-nozzle, high-pressure, pulsed spray cooling in both horizontal and vertical configurations.

II. EXPERIMENTAL SETUP

The novel test bed shown in "Fig. 1" consists of four main assemblies: a pneumatic section, a hydraulic section, a heater section, and a control section. The hydraulic assembly has a high-pressure common rail, 4 BMW Piezoelectric Fuel injectors with SKU: BMW-13538616079, Stainless Steel piping, a 2.5-gallon Bladder Freudenberg Accumulator, a PM 50 GPH Methanol Injection Pump, a 2-gallon reservoir tank, a threeway valve for loading of the coolant. The pneumatic portion uses a high-pressure air tank at 6000 Psi, a pressure regulator, and the same bladder accumulator. The heating comes from 28 Heater Cartridges rated at 1800 W in a 12" square Aluminum Block. The control of the injectors and the heaters is done through a custom-built relay system, coupled with a custom LabVIEW program. To set heating loads, the user specifies two duty cycles for the heating. This is due to the relay distribution being an odd number. Therefore, one power source controls 16 heaters, while the other power source controls 12 heaters. Table 1 shows the duty cycles provided to obtain the experimental heat fluxes.

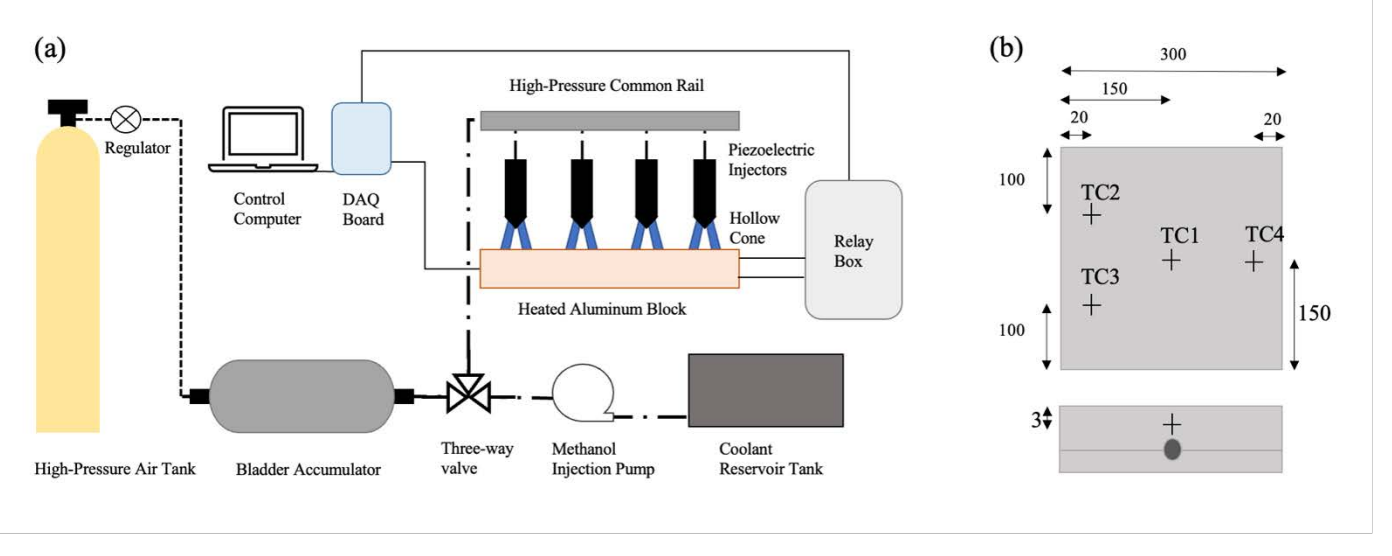


Fig. 1: (a) Schematic of the full test bed. High-pressure air fills the accumulator's bladder increasing the pressure of the coolant. The common rail distributes the coolant into each piezoelectric injector. The control algorithm sets spray parameters of the injectors, while also setting heating conditions for the heaters. (b) Thermocouple locations in millimeters. All sensors are placed 3 mm below the surface

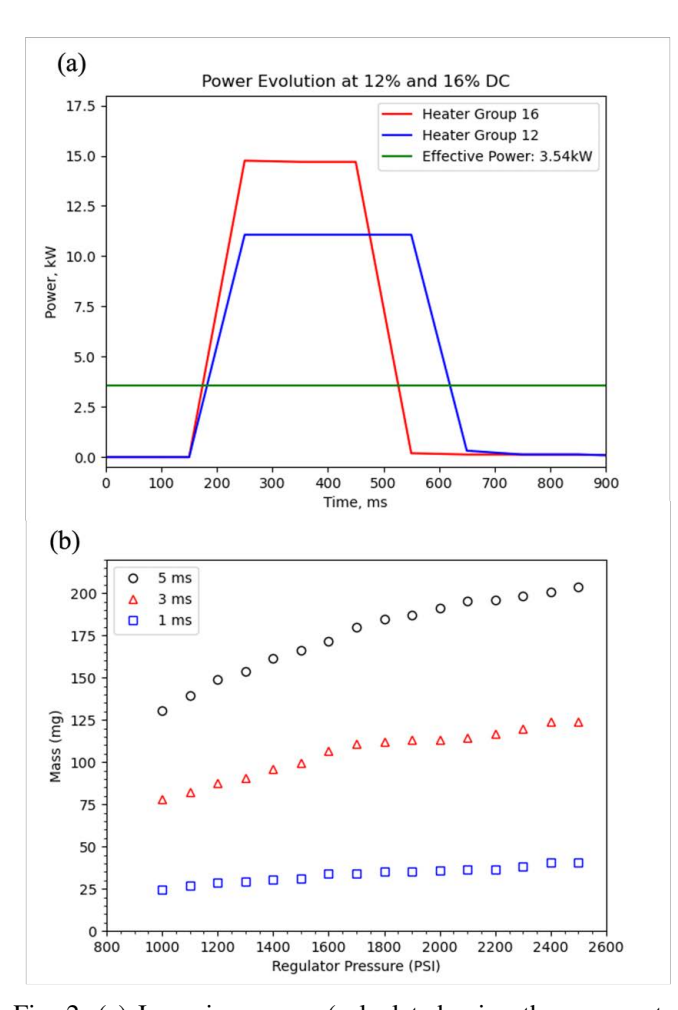


Fig. 2: (a) Incoming power (calculated using the amp meter current) and calculated effective power for a single heating pulse. (b) Ejected mass per pulse at varying spray durations and pressures

TABLE I: Duty Cycle settings for the experimental heat fluxes.

	Experimental Duty Cycles	
Heat Flux (W/cm ²)	Duty Cycle 1	Duty Cycle 2
0.93	3	4
1.86	6	8
2.77	9	12
3.72	12	16
4.66	15	20

To ensure the input power and heat flux of the two sources was equal, amp meters were installed and a LabVIEW monitoring program was established. From the amp meters, the amperage measured 102A, for the 12 heater group, and 136A, for the 16 heater group. Additionally, both power sources measured an AC voltage of 212V using a Fluke 116 True RMS Multimeter. The resulting effective power from each source is 3.54kW per heating pulse shown in "Fig. 2a". Where the effective power calculation is

$$P_{eff} = IV\phi \tag{1}$$

where I is the single source current, V is the outlet voltage, and ϕ is the duty cycle of the heater group.

A proportional-integral (PI) control system was implemented to automate the changes in spray frequency. The algorithm was fed real-time maximum thermocouple data and conducted frequency changes based on the difference between the instantaneous temperature and the set experimental temperature. The coefficients of the proportional and integral controls were -2.0 and 0.03, respectively. Additionally, the actuator saturation was set to 50Hz to keep the controller from operating beyond the hydraulic system's capabilities.

A. Spray Characteristics

To accurately describe the efficiency of a spray cooling system, the characteristics of the spray, such as cone angle, pulse duration, droplet size, and flow rate must be identified. The coolant mass sprayed per pulse was measured at various spray duration and regulator pressure conditions using a JF Series Analytical Balance, displayed in "Fig. 2b". To estimate the incoming flow rate, a constant mass over the spray duration is assumed, leading to the following.

$$\dot{V} = \frac{m_{\text{pulse}}(\tau, P_{\text{reg}}) f_{\text{spray}}}{\rho} \tag{2}$$

Where m_{pulse} is the measured mass at spray duration, τ and spray frequency, f_{spray} , and ρ is the density of the coolant.

The contact radius was estimated through a custom image processing algorithm. A threshold is applied to the droplet image. Edge contours are found and filtered to get those corresponding to only droplets. The hydraulic radius definition is applied to the contours and an average is obtained.

$$R_{h,i} = \frac{2A_{c,i}}{P_{c,i}} \tag{3}$$

Where $A_{c,i}$ and $P_{c,i}$ correspond to the area inside each i-th contour and the perimeter of each i-th contour, respectively.

The cone angle of the spray was calculated from a custom image processing algorithm. A still image of the cone is analyzed. The user selects 4 points on its edges, then these coordinates are used to create 2 vectors that run along the edge of the cone. Using the dot product, the angle between the two vectors is calculated, yielding a result of about 93°.

To ensure that the injectors were spraying at the input frequency, a Phantom Miro c110 was used to measure the time of spraying. Different spraying frequencies were captured using a shadow image configuration. To estimate the spraying frequency, a Fourier transformation of the periodic signal was applied, and the peaks showed the main harmonic.

The results of the cone characterization are viewed in "Fig. 3".

B. Control Experiment

A common method of cooling large areas is through the evaporation of an engineered coolant. To set a benchmark for the pulsed spray cooling technique, a control experiment was carried out which consisted of the following: The aluminum block was heated to a set temperature of 60 °C, 100 mL of water was spread over the hot surface, input heat of 1.86, 2.77, 4.66 W/cm² was applied for 300 seconds (5 minutes) on three iterations per heating load. An illustration of this experiment setup is seen in "Fig. 4a", where the silicone bead is used to hold the stationary water film during the experimental trials.

C. Horizontal Configuration Multiple Sprays

Injectors were placed 2" perpendicular to the heated surface at the center of the block and 3" from the edges. The pressure of the accumulator is set by the pressure regulator located at the exit of the high-pressure air tank. The spray duration is set in the LabVIEW program. For these experiments, the set pressure was 750 psi, and the spray duration was 5ms. The aluminum block was initially heated to a set temperature of

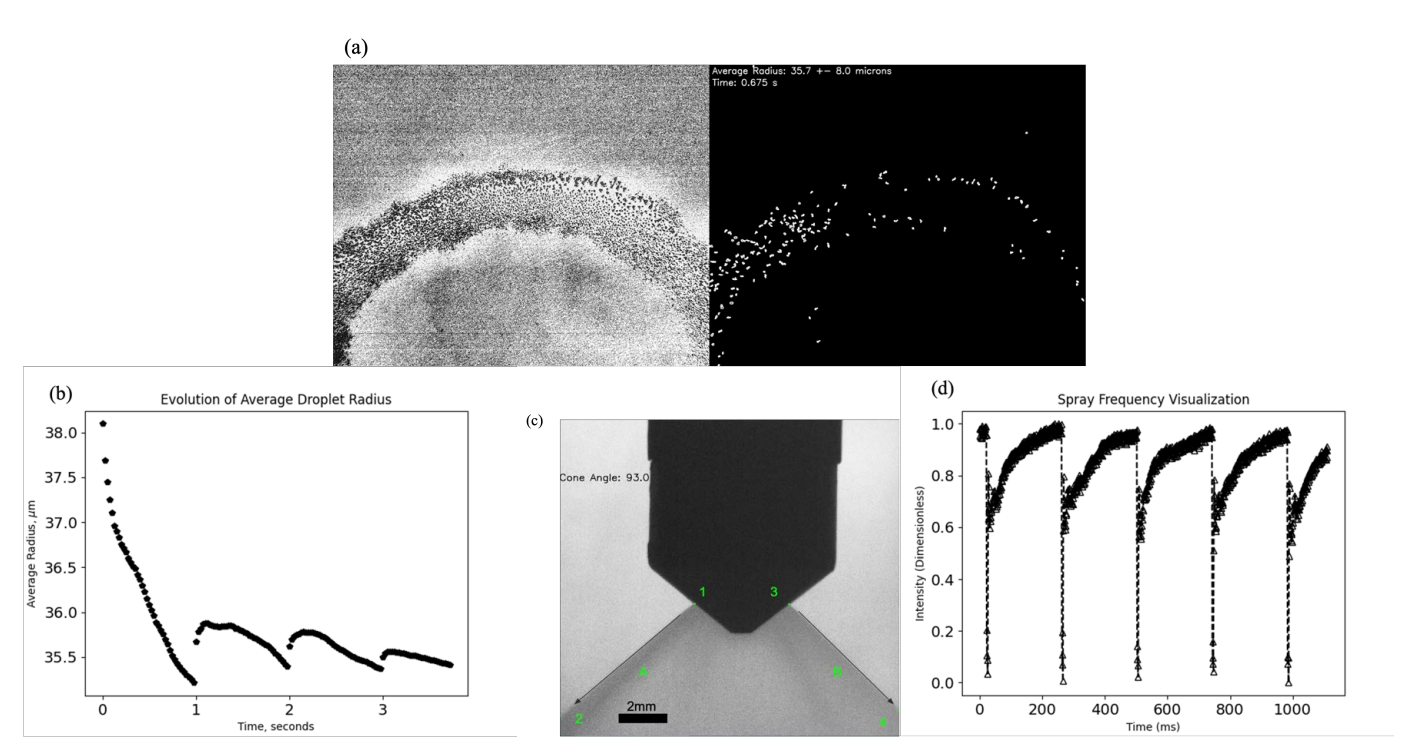


Fig. 3: (a) Grayscale image of the droplet contact-radius distribution of the spray. (b) the evolution of the droplet contact-radius over time. (c) High-speed image of the spray nozzle and cone. (d) Pulse duration verification, non-dimensional spray intensity values with respect to time

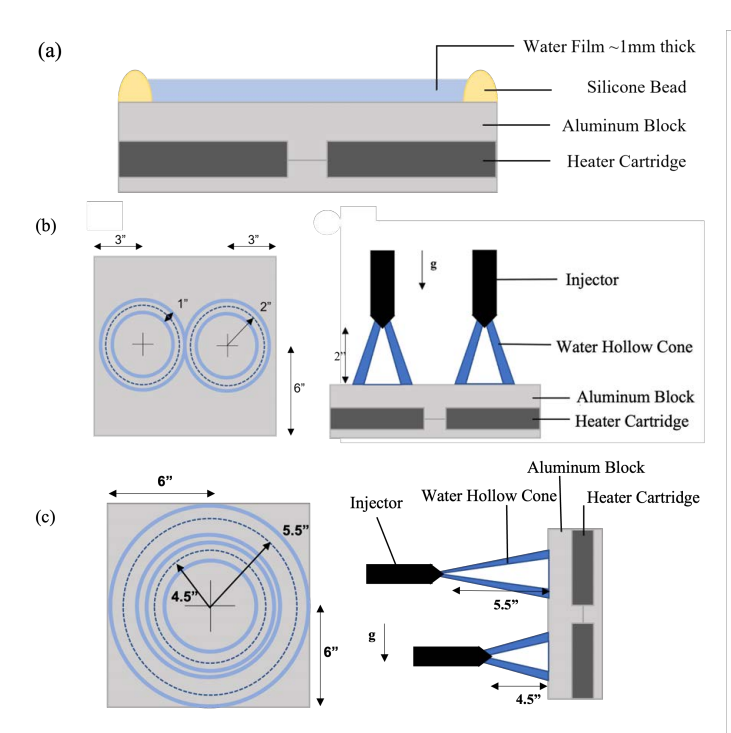


Fig. 4: (a) Sketch of the experimental setup for film evaporation. (b) Ring location of the pulsed sprays and schematic of both piezoelectric injectors impacting the heated surface at a set height of 2" in the horizontal configuration. (c) Concentric ring configuration for the falling film experiments with a set distance from surface of 4.5" and 5.5" for each spray nozzle.

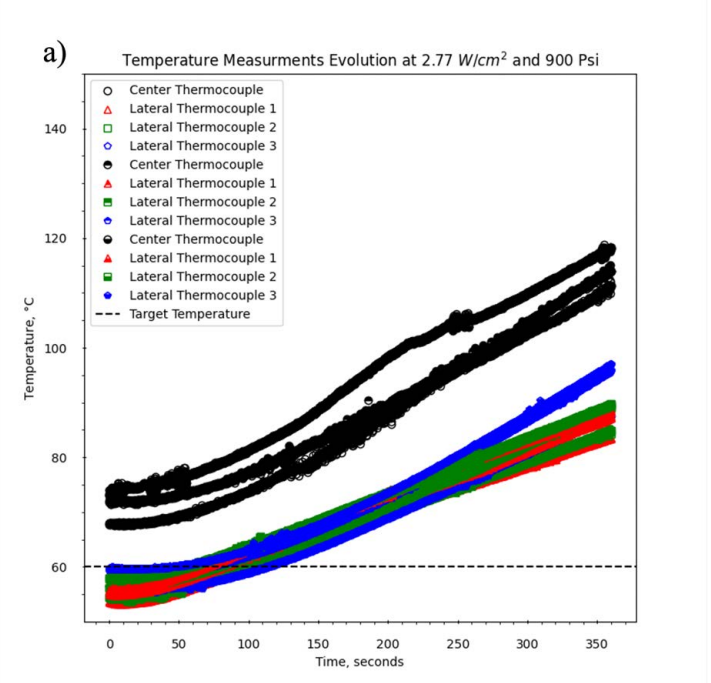
60°C and 90 °C, for each set of experiments. The heating loads used during these sets of experiments were 1.86, 2.79, and 4.66 W/cm². The strategy to accumulate the least amount of static fluid was to start at 1 Hz spraying frequency and increase manually by powers of 2 for every increase in average temperature from the thermocouples. Over the experiment's 5-minute duration, the spraying frequencies were 1, 2, 4, 8, 16, and 32 Hz. A representation of this experimental configuration is seen in "Fig. 4b".

D. Vertical Configuration Multiple Sprays

Given the thermal difficulties from the accumulation of coolant on the surface, the aluminum block was set to its vertical configuration. The motivation for this strategy is to let the excess coolant slide down, capture it on a tray, and measure the average mass flow rate of the non-evaporated coolant shown in figure "Fig. 5b". With these measurements the evaporation efficiency can be calculated for each set temperature, showing where there's a larger ratio of evaporated mass to non-evaporated. The average evaporation efficiency is calculated as follows.

$$\chi_{\text{evap}} = \frac{\dot{m_{in}} - \dot{m_{ne}}}{\dot{m_{in}}} \tag{4}$$

A schematic of the setup is illustrated in "Fig. 4c". The experiments were carried out at a higher pressure of 1500 Psi, while keeping the same 5ms spray duration. The injectors were placed 5.5" away and 4.5" away from the surface.



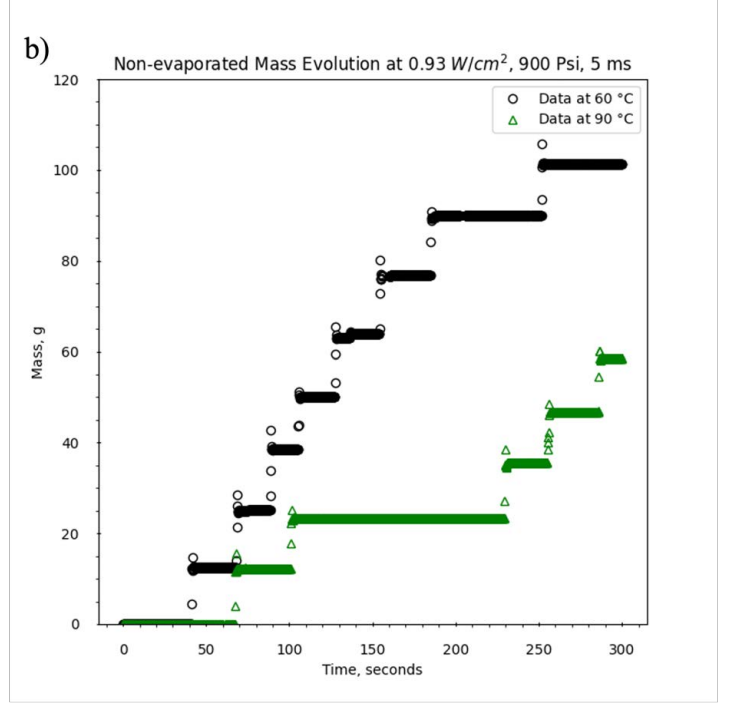


Fig. 5: (a) Thermocouple evolution for all trials in the control experiment with a set temperature of 60°C. (b) Non-evaporated mass evolution at 60 and 90 °C for vertical configuration.

This configuration of the spray injectors allow for more area coverage in the cooling process. The plate was heated to the desired set temperature of 60 °C and 90 °C. For each set temperature, a heating load of 0.93, 1.86, 2.77 and 3.72 W/cm² was applied through the heater cartridges. The water accumulated on the collection tray is weighed on an external scale, JF Series Analytical Balance.

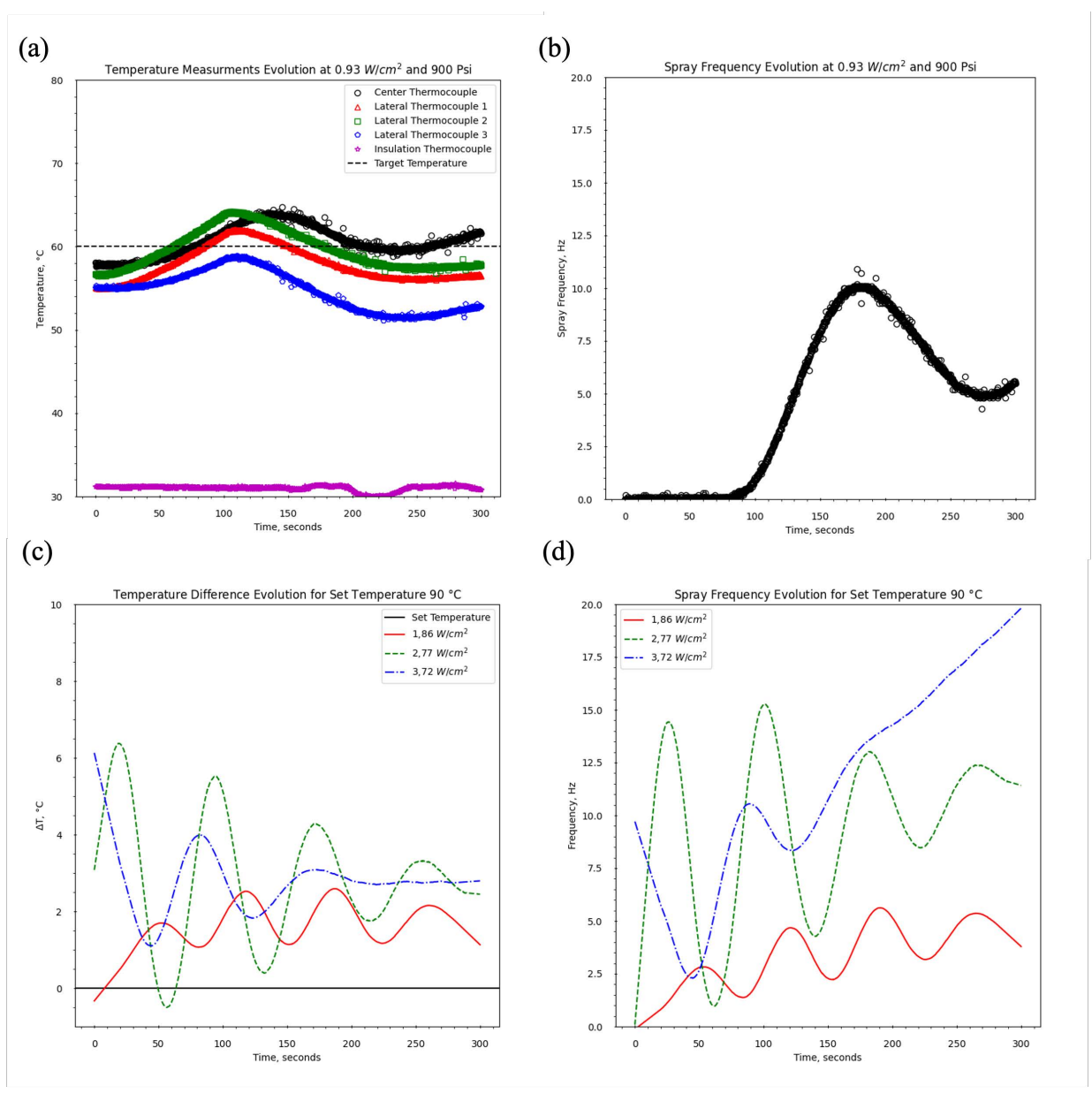


Fig. 6: (a) Temperature evolution in the vertical configuration at 0.93 W/cm² and 60°C. (b) Spray frequency for the vertical setup at 0.93 W/cm² and 60°C. (c) Temperature difference evolution for varying heat fluxes at 90°C. (d) Spray frequency evolution for varying heat fluxes at 90°C

III. RESULTS

Experimental results from the control experiment, film evaporation, show a deficient performance to keep temperatures constant, as seen in "Fig. 5a". Over the span of 360 seconds (about 6 minutes), neither of the thermocouples showed any trend of cooling back down to the initial temperature of 60 °C. Furthermore, the results for all the heating loads show that the center temperature always exceeded water's saturation temperature at 1 atm, of 99.6 °C. With these results as a baseline for evaporation, a comparison can be made between pure film evaporation and pulsed spray cooling.

The results for the horizontal configuration show little control of the surface temperature, for a set temperature of 60 $^{\circ}$ C, all temperatures show increasing trends. This is due to

the accumulation of non-evaporated coolant on the hot surface behaving as insulation. The 90 °C case shows better control over all heating loads. During these experiments, little coolant was left on the surface allowing for higher evaporation rates and thus better temperature regulation.

The vertical configuration results, "Fig. 6" show significantly more control at both set temperatures over all the heating loads. At a set temperature of 90 °C, most experiments reached a steady control spraying frequency with minimal variation in the temperature. However, the highest heating load of 3.72 W/cm², "Fig. 6a and b", shows a rapid increase in the incoming mass flow, suggesting that a prolonged control of temperature at these conditions is not possible. Furthermore, the 0.93 W/cm² case at 60 °C, "Fig. 6c and d", shows small

changes in temperature while keeping a constant spraying frequency, suggesting a successful control in temperature over extended periods.

The non-evaporated mass flow rate results can be viewed in "Fig. 5b". It is immediately apparent that there is a larger non-evaporated mass for 60 °C than 90 °C at almost twice the mass by the end of the experiments. Calculating the average evaporation efficiency from equation 4, we find the efficiencies to be 0.47 and 0.71 for 60 °C than 90 °C, respectively. This calculation sheds light on how much incoming coolant is being used for evaporation (higher cooling capabilities), compared to sensible heating of the coolant.

IV. CONCLUSION

- 1. Film evaporation experiments displayed an increasing trend over the entire experiment for all trials, suggesting that maintaining a constant set temperature is not achievable because of the low evaporation rate of the film.
- 2. Horizontal spraying experiments at a set temperature of 60°C exhibit diverging temperature readings with some indication of stabilizing towards the end of the experiment. However, examining the flow rate measured, it is apparent from the continuously increasing flow rate that no prolonged control of the temperature is achievable, unless higher pressures are employed.
- 3. Horizontal spraying experiments at a set temperature of 90°C shows readings kept between 10°C of the set value for the lowest heat flux. Other heating values showed increasing tendencies in the temperature while also exhibiting increasing flow rate. This pattern indicates that prolonged regulation of the temperature is not possible for heat fluxes above 1.86 W/cm².
- 4. Vertical spraying experiments at a set temperature of 60°C displayed temperatures diverging for heat fluxes above 1.86 W/cm². However, at a heat flux of 0.93 W/cm², temperatures were kept within 2°C of the set value. Additionally, the spraying frequency reaches a constant value of approximately 7 Hz, suggesting a prolonged regulation at this heat flux.
- 5. Vertical spraying experiments at a set temperature of 90°C demonstrates maximum temperature difference of 3°C for heat fluxes up to 2.77 W/cm². For the largest heat flux, the temperature reached a steady state, however, the spraying frequency increased linearly up to the end of the experiment. This result shows that thermal management for a vertical configuration and the set spray parameters can be achieved for extensive operation times bellow 3.72 W/cm².
- 6. To achieve constant temperatures below saturation temperature at higher heat fluxes, pressures above 2000 psi show be used. Furthermore, using the four available piezoelectric injectors will provide greater coverage of the heated plate allowing for more contact area of the coolant with the hot surface.

This work shows the functionality of a novel high-pressure pulsed spray cooling test bed with vertical and horizontal configurations.

Film evaporation experiments displayed an increasing trend over the entire experiment for all trials, suggesting that maintaining a constant set temperature is not achievable because of the low evaporation rate of the film.

Horizontal spraying experiments at a set temperature of 60°C exhibit diverging temperature readings with some indication of stabilizing towards the end of the experiment. However, examining the flow rate measured, it is apparent from the continuously increasing flow rate that no prolonged control of the temperature is achievable, unless higher pressures are employed. Horizontal spraying experiments at a set temperature of 90°C show readings kept between 10°C of the set value for the lowest heat flux. Other heating values showed increasing tendencies in the temperature while also exhibiting increasing flow rate. This pattern indicates that prolonged regulation of the temperature is not possible for heat fluxes above 1.86 W/cm².

Vertical spraying experiments at a set temperature of 60°C displayed temperatures diverging for heat fluxes above 1.86 W/cm². However, at a heat flux of 0.93 W/cm², temperatures were kept within 2°C of the set value. Additionally, the spraying frequency reaches a constant value of approximately 7 Hz, suggesting a prolonged regulation at this heat flux. Vertical spraying experiments at a set temperature of 90°C demonstrates maximum temperature difference of 3°C for heat fluxes up to 2.77 W/cm². For the largest heat flux, the temperature reached a steady state, however, the spraying frequency increased linearly up to the end of the experiment. This result shows that thermal management for a vertical configuration and the set spray parameters can be achieved for extensive operation times bellow 3.72 W/cm².

To achieve constant temperatures below saturation temperature at higher heat fluxes, pressures above 2000 psi should be used. Furthermore, employing the four available piezoelectric injectors will provide greater coverage of the heated plate allowing for more contact area of the coolant with the hot surface.

REFERENCES

- [1] Praveen Kumar Tyagi, Rajan Kumar, and Pranab Kumar Mondal, "A review of the state-of-the-art nanofluid spray and jet impingement cooling", Physics of Fluids 32, 121301 (2020) https://doi.org/10.1063/5.0033503
- [2] K. Oliphant, B.W. Webb, M.Q. McQuay, An experimental comparison of liquid jet array and spray impingement cooling in the non-boiling regime, Experimental Thermal and Fluid Science, Volume 18, Issue 1, 1998, Pages 1-10, ISSN 0894-1777, https://doi.org/10.1016/S0894-1777(98)10013-4.
- [3] D.-Y. Lee, K. Vafai, Comparative analysis of jet impingement and microchannel cooling for high heat flux applications, International Journal of Heat and Mass Transfer, Volume 42, Issue 9, 1999, Pages 1555-1568, ISSN 0017-9310, https://doi.org/10.1016/S0017-9310(98)00265-8.
- [4] Sung, M. K., and Mudawar, I. (April 21, 2009). "Single-Phase and Two-Phase Hybrid Cooling Schemes for High-Heat-Flux Thermal Management of Defense Electronics." ASME. J. Electron. Packag. June 2009; 131(2): 021013. https://doi.org/10.1115/1.3111253
- [5] S.M. Sohel Murshed, C.A. Nieto de Castro, A critical review of traditional and emerging techniques and fluids for electronics cooling, Renewable and Sustainable Energy Reviews, Volume 78, 2017, Pages 821-833, ISSN 1364-0321, https://doi.org/10.1016/j.rser.2017.04.112.